Analysis of brain tissue volume and composition in an extremely-preterm born adolescent cohort

Andrew Melbourne[1], Zach Eaton-Rosen[1], Eliza Orasanu[1], Joanne Beckmann[2], David Atkinson[3] Neil Marlow[2], and Sebastien Ourselin[1]

[1]Centre for Medical Image Computing, University College London, UK. [2]Institute for Women's Health, University College Hospital, London, UK . [3]Centre for Medical Imaging, University College London, UK.

Abstract. The consequences of extremely preterm birth are complex and lifelong. Many studies have begun to link imaging features seen on MRI at or around birth with assessment of neuropsychological and physical function and studies over the last decade have established a comprehensive neonatal neuroimaging phenotype of prematurity. The impact of survival of extremely preterm birth at adolescence is less well known; longitudinal studies begun in the 1990s are now beginning to reveal whether the features seen at early ages persist into adulthood. In this work we assess one such cohort of 19 year-old adolescent survivors of extreme prematurity who underwent a comprehensive neuroimaging assessment. We present early results from this cohort assessing brain volume and we investigate tissue composition of two key regions, the corpus callosum and the thalamus, both regions extensively studied in the neonatal period. We find that brain volume is markedly reduced in the preterm group and that the ratio for grey to white matter remains changed in preterm survivors, relative to their term born peers. Differences are also seen on diffusion-weighted data, T2 relaxometry data and arterial spin labelled imaging.

1 Introduction

The consequences of extremely preterm birth are a global health concern. Rates of prematurity are increasing throughout the world and long-term sequelae range from physical impairments such as cerebral palsy or blindness to social and executive function impairments such as autism. Infants born in extreme prematurity (less than 28 weeks completed gestation) are at increased risk of adverse neurodevelopmental outcome [1] and in the UK, studies have shown that although survival rates at the lowest gestations are increasing, rates of disability remain unchanged [2]. Despite work in a number of preterm cohorts[3, 4], the long-term impact of the effects of extreme prematurity on adolescence are currently poorly understood and the adolescent brain phenotype of extreme prematurity is largely unknown [5]. Neuroimaging studies of young adult survivors are now available and the measurement of tissue composition and structure with MRI can now be correlated with neurocognitive performance. Previous work in preterm neonates

[6, 7] has repeatedly shown developmental differences throughout the thalamus and the white matter and here, through the use of multi-contrast MRI (namely arterial spin labelled MRI, Diffusion-Weighted MRI and T2 relaxometry), we investigate some of the long-term structural and perfusion changes in the brains of survivors of extreme prematurity at 19 years of age.

Our work comprises a study of 69 extremely preterm born 19 year olds and 50 of their age-matched peers, social-economically matched at 6 years of age. Neuroimaging carried out on this cohort enables us to establish the long-term effects of extreme prematurity on the appearance and structure of the brain. This work investigates how brain tissue volumes differ in this extremely preterm born group of young adults and provides a focused analysis of how properties derived from diffusion-weighted imaging data and T2 relaxometry vary within the thalamus and the corpus callosum. Both of these focus regions have been described as notable neurological features of the preterm phenotype on neonatal studies and here we investigate to what extent these difference remain in adolescence.

2 Methods

2.1 Data

Imaging data were acquired for a cohort of 119 adolescents at 19 years of age. Data for 69 extremely preterm (EP) adolescents (F/M=41/28, mean birth gestation= $25.0 \pm 0.8 wks$) and 50 (F/M=30/20) term-born socioeconomically matched peers were acquired on a 3T Phillips Achieva. Diffusion weighted data was acquired across four b-values at b = $0,300,700,2000 s.mm^{-2}$ with n=4,8,16,32 directions respectively at TE=70ms (2.5x2.5x3.0mm). T2 weighted data was acquired in the same space as the diffusion imaging with ten echo times at TE=$13,16,19,25,30,40,50,85,100,150 ms$ (2.5x2.5x3.0mm). We acquired Pseudo-Continuous ASL (PCASL) for 30 control-label pairs with PLD= $1800 ms + 41 ms$/slice, label duration $\tau = 1650 ms$ (resolution 3x3x5mm) [8] Acquisition was carried out using 2D EPI in the same geometry as the DWI ensuring similar levels of distortion. In addition we acquired 3D T1-weighted (TR/TE=6.93/3.14ms) volume at 1mm isotropic resolution. B0 field maps were acquired to correct for EPI-based distortions between the diffusion imaging and the T1-weighted volumes.

2.2 Image Analysis

Tissue segmentation and region labels were obtained using the Geodesic Information Flows framework [9]. This method produces a state-of-the-art segmentation and regional labeling by voxel-wise voting between several propagated atlases guided by the local image similarity. The cerebellum and thalamus region labels in this routine are defined within the propagated atlases. We extract the corpus callosum from the mid-sagittal corpus callosum slice by identification of

the cerebral aqueduct. After manual removal of the fornix we apply an affine transformation followed by a non-rigid (fluid-based) registration algorithm to a common coordinate system. We use the median corpus callosum volume as the representative space [10]. This enables us to investigate local differences in corpus callosum volume and shape within a groupwise coordinate system.

Arterial Spin Labelled MRI Fitting of Cerebral Blood Flow (CBF) maps to ASL data follows the simple derived form for Pseudo-Continuous ASL (PCASL Equation 1) from [8] presented in units of ml/100g/min. Acquisition proceeds by acquiring a number of pairs of control, S_C, and label, S_L, data. Labelled data is generated by positioning a label plane across the carotid arteries. Blood flowing through this label plane is tagged during the acquisition and imaging is carried out after a delay time. Regions of the brain that have received labelled blood have reduce signal proportional to the blood volume that has reached the region. These pairs are averaged to generate single voxel values for the control and label in (1) where λ is the plasma/tissue partition coefficient ($0.9ml/g$), PLD the post-labelling delay between end of bolus and start of imaging, $\mathrm{T1}_{blood}$ the blood T1 value ($1650ms$), α the labelling efficiency (97%) and τ the labelling pulse duration.

$$\mathrm{CBF} = \frac{6000\lambda}{2\alpha} \frac{e^{\mathrm{PLD}/\mathrm{T1}_{\mathrm{blood}}}}{\mathrm{T1}_{\mathrm{blood}}(1 - e^{-\tau/\mathrm{T1}_{\mathrm{blood}}})} \frac{(S_C - S_L)}{S_{PD}} [\mathrm{ml}/100g/\mathrm{min}] \tag{1}$$

Diffusion-Weighted MRI We investigate the spatial microstructure using both the diffusion tensor model and the Neurite Orientation and Density Distribution model (NODDI) model [11]. Tensor fitting is carried out using least-squares fitting to the log of the signal. The resulting 3x3 symmetric matrix system can then be diagonalised to estimate a principal diffusion direction ($\mathbf{p}$) and set of diffusion eigenvalues from which parameters such as the mean diffusivity (MD) and the fractional anisotropy (FA) can be calculated. Multi-compartment model fitting of DWI can also be carried out with NODDI [11]. The diffusion model combines three signal components, A, as a function of b-value, b, and gradient direction $\mathbf{q}$: A single component from an isotropic space, v_{iso}, and a coupled intra- and extra- cellular space represented by the volume fractions v_{in} and v_{ex} with dispersion index γ.

$$S_{dwi}(b, \mathbf{q}) = S_0 \left(v_{in} A_{in}(\gamma, \mathbf{p}) + v_{ex} A_{ex}(\gamma, \mathbf{p}) + v_{iso} e^{-b d_{iso}} \right) \tag{2}$$

T2 Relaxometry We carry out T2 relaxometry and find single component T2 estimates using non-linear least squares fitting of a single exponential decay (3) [12]. Multi-component T2 estimation can be carried out to estimate the volume fractions, v, associated with a set of predefined T2s and extract a short-T2 component that we attribute to myelin water. The thalamic T2 is estimated by fitting a mono-exponential decay to the echo time data greater than 40ms whilst

myelin density, v_{mwf}, can be estimated from the short component of a three-compartment multi-exponential fit to the multi-echo T2 imaging data with T2s of 20,80,200 (4) where $\sum_i v_i = 1$.

$$S_{qT2}(\mathrm{TE}) = S_0 e^{-\mathrm{TE}/\mathrm{T2}} \tag{3}$$

$$S_{qT2}(\mathrm{TE}, \{\mathrm{T2}\}) = S_0 \sum_i v_i e^{-\mathrm{TE}/\mathrm{T2}_i} \tag{4}$$

The measurements of v_{mwf} and v_{in} can be combined to estimate the multi-modal g-ratio, measuring the emergent average internal to external axon diameter ratio, in the preterm corpus callosum using the following expression (5) [7].

$$\mathit{\Gamma} = \left(\frac{v_{mwf}}{(1 - v_{mwf}) v_{in}} + 1 \right)^{-\frac{1}{2}} \tag{5}$$

3 Results

3.1 Brain Volume

Figure 1 shows tissue volume results grouped by EP/term status and by gender. We summarise results for the main tissue classes:

White matter

- White matter volume is between $22.4 - 59.5 cm^3$ (95%ci) lower in preterm females ($371 cm^3 \pm 39.2 cm^3$) than term females ($412 cm^3 \pm 37.5 cm^3$).
- White matter volume is between $40.0 - 47.8 cm^3$ lower in preterm males ($399 cm^3 \pm 46.4 cm^3$) than their term-born counterparts ($464 cm^3 \pm 36.7 cm^3$)
- White matter volume is also significantly lower in term-born females than term-born males ($-29.8 cm^3$ to $-73.3 cm^3$ 95%ci).

Grey matter

- Grey matter volume is between $13.0 - 56.2 cm^3$ (95%ci) lower in preterm females ($565 cm^3 \pm 42.9 cm^3$) than term females ($600 cm^3 \pm 47.6 cm^3$).
- Grey matter volume is between $33.6 - 96.7 cm^3$ lower in preterm males ($610 cm^3 \pm 62.7 cm^3$) than their term-born counterparts ($675 cm^3 \pm 37.1 cm^3$).
- Grey matter volume is also significantly lower in term-born females than term-born males ($-49.1 cm^3$ to $-100 cm^3$ 95%ci).

GM/WM ratio

- The GM/WM ratio is significantly higher (0.03-0.11, p=0.001) in preterm females (1.52 ± 0.09) than in term females (1.45 ± 0.07).
- The GM/WM ratio is also higher (0.02-0.13,p=0.006) in preterm males (1.53 ± 0.09) than in term males (1.46 ± 0.08).
- Differences between preterm males and preterm females (p=0.86) and between term males and term females (p=0.97) are not significant.

Normalisation by brain volume (including ventricular CSF) illustrates how grey, white and cerebellar volume are influenced by total brain volume.

- Differences between grey matter distributions for each group are reduced such that the results no longer reach significance, suggesting that the grey matter proportion is not detectably altered. Differences between normalised cerebellum volumes also do not reach significance.
- Differences between normalised white matter volumes *do* remain significant, suggesting that it is the white matter component that is affected most strongly by extremely preterm birth.

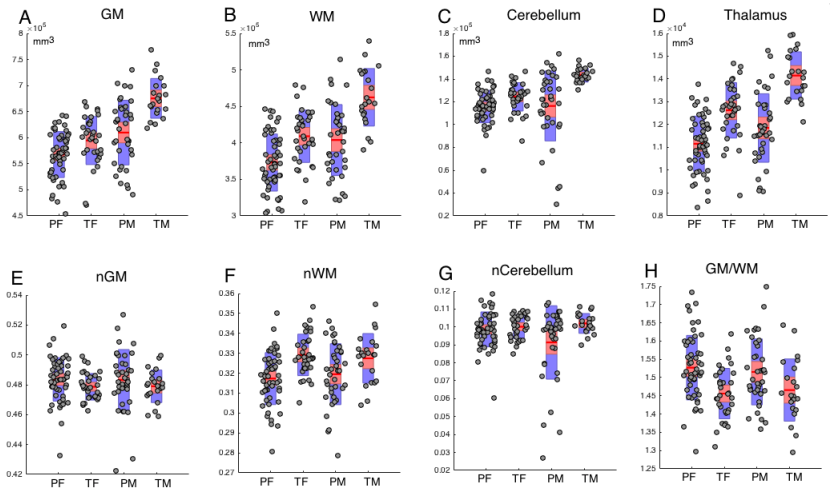

Fig. 1. Tissue volume results found from automatic image segmentation for **top row**: raw tissue volumes in mm^3 and **bottom row**: percentage tissue volumes and grey/white matter ratio. PF=preterm female, TF=term female, PM=preterm male, TM=term male.

3.2 The Thalamus

Figure 2 shows example images and parametric maps for one subject. Figure 3 shows the differences in thalamus volume, average neurite and myelin densities, Fractional Anisotropy (FA), T2 and thalamic blood flow for this cohort.

- Thalamus volume is reduced from an average $13.3 \pm 1.3 cm^3$ to $11.4 \pm 1.3 cm^3$ (ci: -(1.42 to 2.38)cm^3, $p < 0.001$).
- There is non-significant lowering of thalamic FA (p=0.60) in EPs has a significant component associated with a reduced neurite density (ci: -(0.006-0.028), p=0.004).
- There is no observable significant difference in the estimated myelin content (ci: -0.01 to 0.02, p=0.71).
- The average thalamus T2 is reduced from $61.3ms$ to $59.7ms$ (ci: 0.05 to $3.0ms$, p=0.04).
- Thalamus blood flow is reduced on average from 31.5ml/100g/min to 29.7ml/100g/min (ci: -(0.07 to 3.58)ml/100g/min, p=0.04).

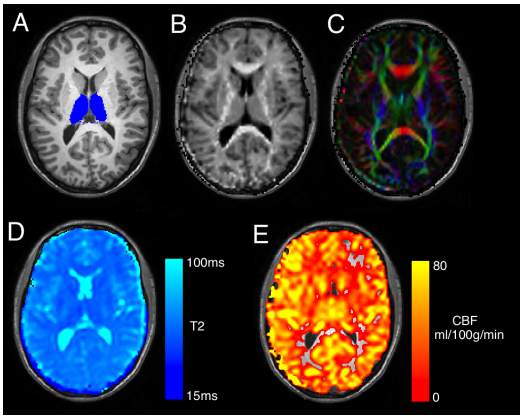

Fig. 2. Example multi-parametric imaging A) T1 weighted image with thalamus segmentation overlaid. B) Neurite density C) colour FA D) T2 map E) CBF map.

3.3 The Corpus Callosum

- The corpus callosum is significantly smaller in preterms ($506 \pm 96 mm^3$) than their term-born peers ($669 \pm 104 mm^3$) (95% ci: -(123-204)mm^3).
- Average mid-sagittal corpus callosum values for the FA are higher in the term group (0.58 ± 0.07) than in the preterm group (0.52 ± 0.10, 95% ci: -(0.02-0.10))

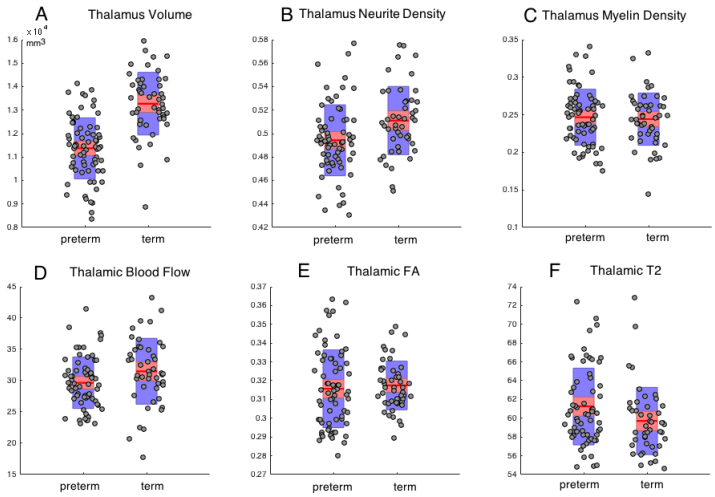

Fig. 3. Summary thalamic imaging data for parameters derived from image segmentation (volumes), diffusion imaging data (Neurite density, FA), T2 relaxometry (myelin density, T2) and arterial spin labelled MRI (blood flow).

- Average T2 is higher at $74.2 \pm 7.4ms$ in the term group than in the preterm group ($88.2 \pm 17.5ms$, 95% ci: (7.9-20.0)ms).
- the intra-axonal and myelin water fractions are both lower (0.51 ± 0.12 / 0.61 ± 0.08 and 0.25 ± 0.05 / 0.29 ± 0.04 respectively 95%ci: -(0.05-0.14) and -(0.02-0.06) respectively) in the preterm group than the term group.
- the measured g-ratio is not significantly different (term=0.77±0.04 preterm=0.77± 0.06, p=0.87),

These results are summarised in the boxplots of Figure 4. We also analysed differences in corpus callosum shape using the results of the non-rigid registration. Figure 5 summarises these results. Within group average segmentations are shown for term controls (Fig 5a) and for extreme-preterms (Fig 5b). Figures 5b and e show the colour coded 2D average absolute deformation (red represents anterior-posterior displacement and green superior-inferior) Finding the Jacobian determinant of the transformations suggests that the major differences in shape arise in the posterior section of the corpus callosum. Figure 5 shows marked thinning of the posterior segment of the main body of the corpus callosum with involvement of the splenium.

4 Discussion

The analysis in this work has allowed a characterisation of the adolescent preterm brain to be made. The results suggest that the white matter component of the

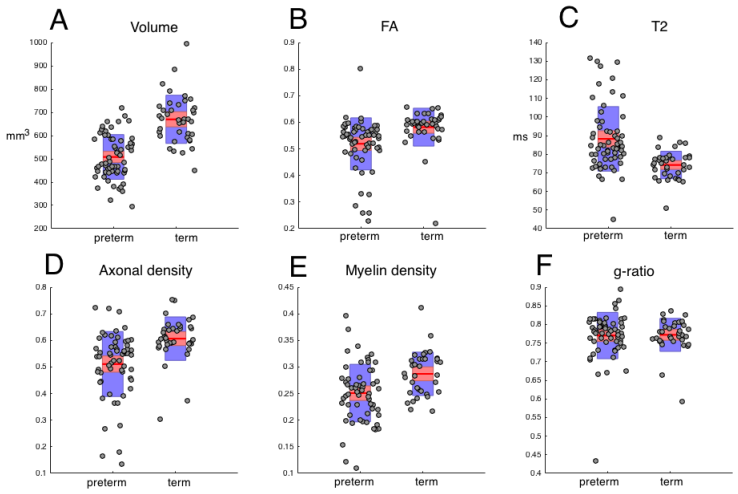

Fig. 4. Summary corpus callosum imaging data for parameters derived from image segmentation (volumes), diffusion imaging data (axonal density, FA), T2 relaxometry (myelin density, T2) and g-ratio (5).

preterm brain is more significantly reduced than the cortical grey and cerebellar volumes. Analysis by both age and gender has allowed us to separate effects due to natural variability in head size from those due to extreme prematurity. Across groups, the most variable results are seen in the EP male group, perhaps suggesting a more variable response to extremely preterm birth. This might be borne out by future studies of neurocognitive function [13].

Using multi-parametric MRI we have compared the phenotypes of the EP and term-born adolescent thalamus. We have shown that the thalamus of extremely preterm survivors shows structural alteration even at 19 years of age. In addition to having a lower volume, the measured neurite density is lower in the EP group, whilst myelin density is not measurably different which may have implications for the functional properties of the tissue. Average thalamus blood flow per voxel and T2 also appear to be reduced. Given the importance of the thalamus as a central relay of information, these features are likely to have strong implications for the social and developmental outcomes of these young adults.

We have also shown that the corpus callosum of extreme preterm survivors remains altered at 19 years of age. Of note, the mid-sagittal corpus callosum area is lower, and remains lower when correcting for an overall lower brain volume in EPs. Notably, the posterior portion of the corpus callosum is most affected, particularly the splenium and this may have a consequence for those areas for which intra-hemispheric communication depends upon this pathway.

Combined, these results suggest comprehensive differences between the appearance of the brain of survivors of extreme preterm birth and their term-born peers. Most striking is the observation that the white matter component is most

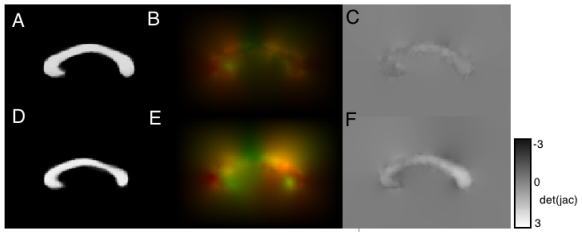

Fig. 5. Corpus callosum shape analysis for A/D, average preterm and term corpus callosums respectively; B/E colour-coded (absolute) displacement fields (red=AP green=SI displacement) and C/F Jacobian determinant maps showing disproportionate posterior deformations between term and preterm groups.

affected by prematurity, volumes are reduced proportionately irrespective of absolute brain volume. This feature is consistent with observations from previous studies [13, 3]. This feature may go some way to explaining some of the difference in outcome between these groups. The global change in white matter proportion is backed up to some extent by the measurements of tissue composition made from relaxometry, ASL and DWI. In addition to having reduced volume, the corpus callosum appears to have reduced FA, and reduced axonal and myelin density coupled with increased T2 and these features seem to be most related to the posterior third of the structure. In addition to the white matter alterations seen in the global white matter and corpus callosum, thalamus volume is also reduced, although the changes in tissue composition appear to be less striking than in the corpus callosum; white matter differences may be the key detectable feature of extreme prematurity.

Our future work will investigate to what extent structural and functional measurement differences in the thalamus are linked to external physiological and psychological factors and investigate how the observation of a relative white matter reduction reveals itself on microstructural imaging and how these features manifest in neuropsychological examinations. Work such as this, characterising the extremely preterm brain phenotype at adolescence is crucial for understanding the long term impact on structural appearance.

Acknowledgements We would like to acknowledge the MRC (MR/J01107X/1), the National Institute for Health Research (NIHR), the EPSRC (EP/H046410/1) and the National Institute for Health Research University College London Hospitals Biomedical Research Centre (NIHR BRC UCLH/UCL High Impact Initiative BW.mn.BRC10269). This work is supported by the EPSRC-funded UCL Centre for Doctoral Training in Medical Imaging (EP/L016478/1).

References

1. Volpe, J.J.: Brain injury in premature infants: a complex amalgam of destructive and developmental disturbances. Lancet Neurol **8**(1) (Jan 2009) 110–124
2. Moore, T., Hennessy, E.M., Myles, J., Johnson, S.J., Draper, E.S., Costeloe, K.L., Marlow, N.: Neurological and developmental outcome in extremely preterm children born in england in 1995 and 2006: the epicure studies. BMJ **345** (2012) e7961
3. Keunen, K., Kersbergen, K.J., Groenendaal, F., Isgum, I., de Vries, L.S., Benders, M.J.N.L.: Brain tissue volumes in preterm infants: prematurity, perinatal risk factors and neurodevelopmental outcome: a systematic review. J Matern Fetal Neonatal Med **25 Suppl 1** (Apr 2012) 89–100
4. Zubiaurre-Elorza, L., Soria-Pastor, S., Junque, C., Sala-Llonch, R., Segarra, D., Bargallo, N., Macaya, A.: Cortical thickness and behavior abnormalities in children born preterm. PLoS One **7**(7) (2012) e42148
5. Cheong, J.L.Y., Anderson, P.J., Roberts, G., Burnett, A.C., Lee, K.J., Thompson, D.K., Molloy, C., Wilson-Ching, M., Connelly, A., Seal, M.L., Wood, S.J., Doyle, L.W.: Contribution of brain size to iq and educational underperformance in extremely preterm adolescents. PLoS One **8**(10) (2013) e77475
6. Eaton-Rosen, Z., Melbourne, A., Orasanu, E., Cardoso, M.J., Modat, M., Bainbridge, A., Kendall, G.S., Robertson, N.J., Marlow, N., Ourselin, S.: Longitudinal measurement of the developing grey matter in preterm subjects using multi-modal mri. Neuroimage **111** (May 2015) 580–589
7. Melbourne, A., Eaton-Rosen, Z., Orasanu, E., Price, D., Bainbridge, A., Cardoso, M.J., Kendall, G.S., Robertson, N.J., Marlow, N., Ourselin, S.: Longitudinal development in the preterm thalamus and posterior white matter; mri correlations between diffusion weighted imaging and t2 relaxometry. Human Brain Mapping **37(7)** (2016) 2479–2492
8. Alsop, D.C., Detre, J.A., Golay, X., Gnther, M., Hendrikse, J., Lu, H., Macintosh, B.J., Parkes, L.M., Smits, M., van Osch, M.J.P., Wang, D.J.J., Wong, E.C., Zaharchuk, G.: Recommended implementation of arterial spin-labeled perfusion mri for clinical applications: A consensus of the ismrm perfusion study group and the european consortium for asl in dementia. Magn Reson Med (Apr 2014)
9. Cardoso, M.J., Modat, M., Wolz, R., Melbourne, A., Cash, D., Rueckert, D., Ourselin, S.: Geodesic information flows: spatially-variant graphs and their application to segmentation and fusion. IEEE TMI **99** (2015)
10. Cahill, N.D., Noble, J.A., Hawkes, D.J.: Fourier methods for nonparametric image registration. In: IEEE Conference on Computer Vision and Pattern Recognition. (2007) 1–8
11. Zhang, H., Schneider, T., Wheeler-Kingshott, C.A., Alexander, D.C.: Noddi: practical in vivo neurite orientation dispersion and density imaging of the human brain. Neuroimage **61**(4) (Jul 2012) 1000–1016
12. Dingwall, N., Chalk, A., Martin, T.I., Scott, C.J., Semedo, C., Le, Q., Orasanu, E., Cardoso, J.M., Melbourne, A., Marlow, N., Ourselin, S.: T2 relaxometry in the extremely-preterm brain at adolescence. Magnetic Resonance Imaging **34(4)** (2016) 508–514
13. Northam, G.B., Ligeois, F., Chong, W.K., Wyatt, J.S., Baldeweg, T.: Total brain white matter is a major determinant of iq in adolescents born preterm. Ann Neurol **69**(4) (Apr 2011) 702–711